



**HAL**  
open science

# Experimental and Thermodynamic Study of Tantalum-containing Iron-base Alloys reinforced by Carbides: Part I-case of (Fe, Cr)-base ferritic steels

P. Berthod, Y Hamini, L. Aranda, L Héricher

## ► To cite this version:

P. Berthod, Y Hamini, L. Aranda, L Héricher. Experimental and Thermodynamic Study of Tantalum-containing Iron-base Alloys reinforced by Carbides: Part I-case of (Fe, Cr)-base ferritic steels. *Calphad*, 2007, 10.1016/j.calphad.2007.01.007 . hal-02406116

**HAL Id: hal-02406116**

**<https://hal.science/hal-02406116>**

Submitted on 12 Dec 2019

**HAL** is a multi-disciplinary open access archive for the deposit and dissemination of scientific research documents, whether they are published or not. The documents may come from teaching and research institutions in France or abroad, or from public or private research centers.

L'archive ouverte pluridisciplinaire **HAL**, est destinée au dépôt et à la diffusion de documents scientifiques de niveau recherche, publiés ou non, émanant des établissements d'enseignement et de recherche français ou étrangers, des laboratoires publics ou privés.

# Experimental and Thermodynamic Study of Tantalum-containing Iron-base Alloys reinforced by Carbides: Part I-case of (Fe, Cr)-base ferritic steels

P. Berthod\*, Y. Hamini, L. Aranda, L. Hélicher

Laboratoire de Chimie du Solide Minéral (UMR 7555), Université Henri Poincaré

BP 239, 54506 Vandoeuvre-lès-Nancy – France

\* Corresponding author's e-mail : patrice.berthod@centraliens-lille.org

\* Corresponding author's telephone number: (33) 3 83 68 46 66

and fax number: (33) 3 83 68 46 11

Post-print version of the article *Calphad*, Vol. 31, pp. 351-360 (2007); doi:10.1016/j.calphad.2007.01.007

**Abstract.** Experiments and thermodynamic calculations were performed on three iron-base alloys containing 30 wt.% of chromium and 3 to 6 wt.% of tantalum. Solidus temperatures, natures and surface fractions of all phases present after an exposure for 50 hours at 1000°C, 1100°C and 1200°C, were determined for each alloy. These results were compared to values calculated using Thermo-Calc. Two alloys display solidus temperatures above 1400°C, while all the liquidus temperatures are higher than 1500°C. Tantalum carbides are present with high fractions, compared to similar Co-base and Ni-base alloys. Their observation and quantification using electron microscopy micrographs and image analysis may lead to overestimate the surface fractions of TaC. Calculations of carbide fractions from the chemical composition of matrix is to be preferred. A precipitation of coarse chromium carbides may occur for 1100°C and 1200°C.

**Keywords:** Iron-based alloys; Tantalum carbides; Chromium carbides; Experimental characterization; Thermodynamic modeling

## 1. Introduction

At high temperatures the carbide phases are of a great importance for some superalloys since they allow them to reach a sufficient mechanical strength to resist creep flow or static stresses to which these alloys can be exposed in service [1,2]. When a good resistance against high temperature corrosion is also required, superalloys must contain a high amount of chromium which can lead to the existence of chromium carbides. Other carbides may exist when other carbides-forming elements are also present in the composition, like tantalum which can induce the apparition of TaC carbides.

The mechanical behavior of such alloys at high temperature depends on the initial carbide fractions as well as on the fraction of carbides after a long exposure at high temperature. In some cases a piece working at high temperature is exposed to a unique temperature. But more generally temperature is not homogeneous in the whole piece. Therefore it could be useful to have a good knowledge of the microstructure at different temperatures, but also to own a tool allowing a quantitative prediction of microstructures at all the intermediate temperatures. In addition, the elaboration by casting of the alloys is more or less difficult depending on the melting temperature range, and both liquidus and solidus temperatures are very useful indications to succeed in the melting of the alloy and in the filling of the mold before solidification.

The topic of this work is first to provide, for three temperatures above 1000°C, microstructure results for three iron-base superalloys containing tantalum and

strengthened by chromium carbides and/or tantalum carbides. Second, the refractoriness and melting range are determined by measurements of both solidus and liquidus temperatures. All these data can be helpful to evaluate databases that are candidates for thermodynamic calculations on such alloys and to improve them when mismatches are observed. A first evaluation was performed on a database which does not contain all the descriptions of the sub-systems of the quaternary Fe-Cr-C-Ta.

## **2. Experimental method**

### *2.1. Elaboration of the alloys*

All the studied alloys contain about 30wt.% of chromium which allows them to display a chromia-forming behavior for a good resistance at high temperature against both oxidation by air and corrosion by molten substances. Tantalum is also present in all alloys, with two targeted contents: 3wt.% for the FETA1 and FETA2 alloys, and 6wt.% for the FETA3 alloy. Tantalum may form carbides with carbon which is present in the three alloys: 0.2wt.% for FETA1 and 0.4wt.% for the two other alloys. All alloys were elaborated from pure elements (>99%, Alfa Aesar), by casting in a high frequency induction furnace (CELES), under an atmosphere of 300mbar of argon gas. Solidification was achieved in the water-cooled copper crucible of the furnace, and led to compact ingots of nearly 100g. Thereafter, the stresses that may appear during solidification or during the cooling down to room temperature, were released with a short heat treatment. The latter was achieved in a tubular resistive furnace, with a heating rate of 20°C/min, an isothermal stage at 1000°C for about 2 hours, and a slow cooling at less than 5°C/min. Cutting the ingots allowed to obtain samples for tests. The dimensions of the two types of samples were approximately 2 x 2 x 8 mm<sup>3</sup> for thermal analysis tests and 10 x 10 x 3 mm<sup>3</sup> for high temperature exposures.

### *2.2. Metallographic preparation, microstructure observations and global chemical composition determination*

The microstructures of the alloys were observed, on one hand after casting and stress-releasing treatment and on the other hand after each high temperature exposure. A cold resin (Araldite CY230 +Strengthener Escil HY956) was poured around the cut samples. They were then polished, first with SiC paper from 120 to 1200 grid under water, and second with 1µm diamond pastes. Metallographic observations were done using a XL30 Philips Scanning Electron Microscope (SEM), mainly in the Back Scattered Electrons mode (BSE) and with an acceleration voltage of 20kV. The chemical composition of each alloy was determined using the Energy Dispersion Spectrometry (EDS) device of the SEM, to know the obtained Fe, Cr and Ta contents (carbon cannot be analyzed by EDS). This was done on five randomly selected areas, each of about 0.17mm<sup>2</sup>, and the average value was calculated.

### *2.3. Thermal analysis measurements*

Differential Thermal Analysis (DTA) were performed on the alloys to determine both solidus and liquidus temperatures (when possible). The heating rate was 20 °C/min

up to 1200 °C, then 5 °C/min up to 1500 °C which is the maximal temperature allowed by the apparatus. This was followed by a cooling at 5 °C/min down to 1200°C, then 20 °C/min down to room temperature. Beginnings and ends of fusion and solidification were measured on the heating part and on the cooling part. They were considered to be the temperatures at which the temperature evolution becomes not linear with time (beginnings of fusion and of solidification) or on the contrary becomes linear again (ends of fusion and of solidification). The solidus and liquidus temperatures were determined as being the values obtained on the heating curve. But the average value of the temperatures of the beginning (resp. end) of fusion and of the end (resp. beginning) of solidification were also considered.

#### 2.4. High temperature treatments, carbides identification, matrix compositions and phase surface fractions

Three samples of each alloy were exposed for 50 hours to three different temperatures (1000, 1100 and 1200 °C). Exposures were performed in a high temperature furnace with a heating rate of 20 °C/min and a cooling rate of 10 °C/min.

Thereafter, the samples for microstructure observations were cut in two parts, using an Isomet 5000 saw, for the preparation of samples for metallographic observations. The natures of the carbides that appeared in the alloys were identified using Wavelength Dispersion Spectrometry (WDS) with a CAMECA SX100 microprobe. The matrix compositions were also determined using the same WDS apparatus, on five different locations with calculation of the average values of all contents.

The volume fractions of carbides were determined following two ways. The first way consisted in taking pictures on each alloy exposed to high temperature, using the SEM in BSE mode with a magnification of x500. This was performed on five different locations randomly selected (areas of 0.04mm<sup>2</sup>). The BSE mode, for which the average atomic number induces different levels of gray, allowed the separation of matrix (gray), chromium carbides (dark) and tantalum carbides (white). Thereafter the surface fractions of all phases were measured using the Photoshop CS software of Adobe. Each surface fraction is thus the average of five measures, and were assumed to be close to the volume fractions.

The second way consisted in calculating mass fractions of Cr<sub>23</sub>C<sub>6</sub> and TaC (noted  $f_w[\text{Cr}_{23}\text{C}_6]$  and  $f_w[\text{TaC}]$ ) from the mass fraction of matrix ( $f_w[\text{mat}]$ ), and respectively from:

- the analyzed Cr weight contents of the matrix ( $W_{\text{Cr}}[\text{mat}]$ ) and of the whole alloy ( $W_{\text{Cr}}[\text{all}]$ ), and the theoretical Cr weight content of the Cr<sub>23</sub>C<sub>6</sub>-carbides ( $W_{\text{Cr}}[\text{Cr}_{23}\text{C}_6]=0.943$ ), according to equation (1),

- the analyzed Ta weight contents of the matrix ( $W_{\text{Ta}}[\text{mat}]$ ) and of the whole alloy ( $W_{\text{Ta}}[\text{all}]$ ), and the theoretical Ta weight content of the TaC-carbides ( $W_{\text{Ta}}[\text{TaC}]=0.938$ ), according to equation (2),

$$f_w[\text{Cr}_{23}\text{C}_6] = \frac{W_{\text{Cr}}[\text{all}] - f_w[\text{mat}] \times W_{\text{Cr}}[\text{mat}]}{W_{\text{Cr}}[\text{Cr}_{23}\text{C}_6]} \quad (1)$$

$$f_w[\text{TaC}] = \frac{W_{\text{Ta}}[\text{all}] - f_w[\text{mat}] \times W_{\text{Ta}}[\text{mat}]}{W_{\text{Ta}}[\text{TaC}]} \quad (2)$$

in which  $f_w[\text{mat}]$  is calculated according equation (3):

$$f_w[\text{mat}] = \frac{1 - \left( \frac{W_{\text{Cr}}[\text{all}]}{W_{\text{Cr}}[\text{Cr}_{23}\text{C}_6]} + \frac{W_{\text{Ta}}[\text{all}]}{W_{\text{Ta}}[\text{TaC}]} \right)}{1 - \left( \frac{W_{\text{Cr}}[\text{mat}]}{W_{\text{Cr}}[\text{Cr}_{23}\text{C}_6]} + \frac{W_{\text{Ta}}[\text{mat}]}{W_{\text{Ta}}[\text{TaC}]} \right)} \quad (3)$$

Thereafter the corresponding volume fractions were calculated according to equation (4):

$$f_v[\phi_j] = \frac{f_w[\phi_j]}{\rho_{\phi_j}} / \sum_i \left( \frac{f_w[\phi_i]}{\rho_{\phi_i}} \right) \quad (4)$$

in which  $f_v[\phi_j]$ ,  $f_w[\phi_j]$  and  $\rho_{\phi_j}$  are respectively the volume fraction, the weight fraction and the density of the phase  $\phi_j$ . The values used for the densities (expressed in  $\text{g.cm}^{-3}$ ) are 7.6 for matrix (as given in [3] for ferritic steels and verified by direct measurement on samples), 6.941 for  $\text{Cr}_7\text{C}_3$ , 6.953 for  $\text{Cr}_{23}\text{C}_6$  and 14.5 for TaC [4].

## 2.5. Thermodynamic calculations

Calculations were performed for the three alloys with the Thermo-Calc software [5] and the database SSOL (SGTE) [6]. This database already contained the descriptions of the following binary and ternary systems: Fe-C [7], Fe-Cr [8], C-Cr [9] and Fe-C-Cr [10]. It was supplemented with the descriptions of two other systems: Ta-C [11] and Ta-Cr [12]. Thermo-Calc calculations were performed for each alloy from the chemical compositions determined by EDS measurements on the obtained alloys. The following quantities were calculated:

- the solidus temperature and the liquidus temperature,
- the natures of the phases present at 1000 °C, 1100 °C and 1200 °C, and their mass fractions that were converted into volume fractions according to equation (4),
- the chemical composition of matrix.

## 3. Results

### 3.1. Initial microstructures and chemical compositions

Figure 1 shows the initial microstructures of the three alloys. Primary carbides, which appeared during solidification, can be seen in grain boundaries for all alloys. They are exclusively tantalum carbides (white in BSE mode), with the TaC stoichiometry as shown by the WDS microprobe spot measures. Even for a low carbon content (FETA1), these tantalum carbides are present and they form an interdendritic network which is almost continuous. Some secondary TaC carbides can be also observed and they probably began to appear during the stress-releasing treatment. The

TaC density of the FETA2 alloy is similar to the previous alloy, even if its carbon content is the double. However more carbon led to the appearance of another type of carbide, darker than the matrix. The FETA3 alloy is very different from the two previous alloys: tantalum carbides are present in significantly higher amounts and they seem to form a continuous eutectic with the matrix along the interdendritic areas.

The chemical compositions obtained for the three alloys by EDS measurements are given in Table 1 (**in bold characters**) where the targeted compositions are remembered for comparison. The chromium contents were always well respected while the tantalum contents are lower than the targeted values for the FETA1 and FETA2 alloys but a little higher than 6% for the FETA3 alloy. It was not possible to obtain a sufficiently accurate value of the carbon content for the alloys, even by using microprobe. But the targeted value can be considered well respected here since the elaboration mode is the same as for previous similar alloys for which the obtained carbon content was exactly the targeted one.

### 3.2. *Solidus and liquidus temperatures*

Differential Thermal Analysis experiments were carried out on the three alloys. For the assessment of the solidus temperature, the beginning of fusion (heating part of the curve) was first considered. The average temperature of the beginning of fusion and the end of solidification, respectively for heating and cooling, was also determined. Unfortunately it was never possible to obtain the liquidus temperature since fusion was never finished when the temperature reached the maximum value allowed by the apparatus (about 1500°C). As an example Figure 2 displays the DTA curve obtained on the FETA2 alloy while Table 2 shows the values of solidus temperatures determined for the three alloys, according to the two methods: during heating (**in bold characters**) and average value between heating and cooling (**in bold and italic characters**).

The solidus temperatures are all very high (more than 1300°C), notably for the FETA1 and FETA3 alloys for which they are near 1400°C. The liquidus temperatures were never measured but there are all higher than 1500°C since total fusion was never experimentally achieved.

### 3.3. *Microstructure after exposures to high temperature*

Figures 3, 4 and 5 respectively displays some selected BSE images of the FETA1, FETA2 and FETA3 alloys after exposure for 50 hours at 1000, 1100 and 1200°C. In most cases new microstructures have evolved in order to more correspond to the equilibrium state at the applied temperature.

For the alloy FETA1, there is no real difference between the microstructure after stress-releasing heat treatment (done at 1000°C too) and the microstructure after exposure for 50 hours at 1000°C. However one can note that secondary TaC carbides became more compact and rounder during this exposure in order to reduce the interfacial energy. For the heat treatment at 1100°C, primary carbides are less present in the structure while some secondary carbides have disappeared. After 50 hours at 1200°C, the microstructure has evolved significantly: the morphology of the TaC carbides is totally different (some of them are more elongated) since acicular dark chromium carbides have appeared. WDS spot analysis that was often difficult because

of the too small size of carbides. However it showed that there are probably  $\text{Cr}_{23}\text{C}_6$  carbides since their atomic ratio  $\%_{\text{at}}\text{M} / \%_{\text{at}}\text{C}$  is close to 4 or higher.

Like for the previous alloy, the microstructure of FETA2 after 50 hours at  $1000^\circ\text{C}$  remains quite similar to the initial one. For  $1100^\circ\text{C}$  the tantalum carbides seem to be broken and more dispersed. After 50 hours at  $1200^\circ\text{C}$ , they are rounder and more dispersed while their surface fraction seems to have drastically decreased. New chromium carbides, darker than the previous ones and with an acicular morphology, have appeared. One can think that they are maybe  $\text{Cr}_7\text{C}_3$  carbides since they are darker than the  $\text{Cr}_{23}\text{C}_6$  that existed at  $1000^\circ\text{C}$  and  $1100^\circ\text{C}$  in the alloy, and their atomic ratio  $\%_{\text{at}}\text{M} / \%_{\text{at}}\text{C}$  is sensibly lower than for  $\text{Cr}_{23}\text{C}_6$ . Here too they were too small to allow a good stoichiometry determination with the microprobe.

The microstructure of the FETA3 alloy after heat treatment at  $1000^\circ\text{C}$  is also quite similar to the initial one. Eutectic tantalum carbides are very dense in the interdendritic spaces and a precipitation of secondary TaC carbides in matrix has occurred during the high temperature exposition. After 50 hours at  $1100^\circ\text{C}$ , dark chromium carbides, sometimes very coarse, have appeared throughout the matrix. WDS analysis showed that they are probably  $\text{Cr}_{23}\text{C}_6$  carbides. Observations on the sample exposed to  $1200^\circ\text{C}$  led to same results: the main difference was the reduction of the apparent fraction of the TaC phase, by comparison to  $1100^\circ\text{C}$ .

Five pictures were randomly taken on each alloy for each temperature with the MEB in BSE mode. Table 3 presents the results of the image analysis performed on these pictures, i.e. the average value +/- standard deviation (**in bold characters**). At  $1000^\circ\text{C}$ , FETA1 and FETA3 only contain tantalum carbides, while FETA2 also contains chromium carbides (since its carbon content is higher than for FETA1 for the same Ta content). Surprisingly, image analysis led to higher values of TaC surface fractions in the FETA1 alloy than in the FETA2 alloy at  $1000^\circ\text{C}$ , and to similar surface fraction as in the FETA3 alloy for  $1000^\circ\text{C}$ . However, it can be seen on micrographs that the surface fraction of the TaC phase in the FETA1 alloy is on the contrary quite similar to the one of the FETA2 alloy and not so high as for the FETA3 alloy. The latter alloy contains more TaC carbides than the two other alloys (except for FETA1 at  $1000^\circ\text{C}$ ), because of its high amount of tantalum. The TaC surface fractions of all alloys decrease when temperature increases while it is the contrary for the chromium carbides, as qualitatively shown before.

#### *3.4. Chemical compositions of the alloys matrix*

Table 4 displays the chemical compositions of the matrix of the alloys for the three temperatures (average values of 5 WDS spot analysis performed with microprobe, **in bold characters**). The matrix seems to never contain carbon since the content is often zero or the standard deviation is of the same order of magnitude as the average value. An exception is the FETA2 alloy which contains a significant (but low) quantity of carbon at  $1000^\circ\text{C}$ . Tantalum is never significantly present in the FETA1 and FETA2 alloys. A very small quantity of tantalum seems to exist in solid solution in the FETA3 matrix at  $1100$  and  $1200^\circ\text{C}$  since the average value is sensibly higher than the standard deviation. On the contrary chromium contents of around 30wt.% are present in all alloys.

Thus, generally tantalum and carbon seem to have exclusively formed carbides, either interdendritic or secondary precipitated in the matrix, and are not present in the matrix.

#### 4. Comparisons with thermodynamic calculations

##### 4.1. Computed solidus and liquidus temperatures

Thermodynamic calculations were all performed from the obtained chemical compositions given in Table 1. The obtained solidus and liquidus temperatures are added in Table 2 for comparison with the experimental DTA measures. There is a significant mismatch between the experimental values and the calculated ones, especially for the FETA3 alloy for which the tantalum content is particularly high. Liquidus temperatures calculated using Thermo-Calc are all higher than 1500°C, i.e. the maximal temperature reached for the DTA experiments that was never high enough to obtain the totally liquid alloys. This is qualitatively in good agreement between calculations and experiment. In addition, calculations also show that liquidus temperature should increase with both the carbon content and the tantalum content.

##### 4.2. Computed matrix chemical compositions

Table 4 displays the chemical compositions obtained from Thermo-Calc calculations for the matrix of each alloy for all exposure temperatures, as well as the measured contents. Calculations show that the chromium content is always around 30wt.%, whatever the alloy and the considered temperature. The calculated tantalum contents are very low for all alloys (compared to the alloy contents of 3 and 6wt.%Ta). The matrix of the Ta-richest alloy, FETA3, logically contains more tantalum than the two others. The carbon contents are very low (but they can reach the quarter of the total content of the alloy) and increase with temperature. For a given temperature, the FETA2 matrix contains more carbon than the two other matrixes.

The calculated Cr contents are generally in good agreement with values obtained by WDS analysis. The calculated Ta contents are generally higher than the WDS results, even if calculated values sometimes remain in the relatively large intervals of uncertainty of WDS results. Moreover, calculated Ta contents are significantly higher than WDS measures for FETA3 at all temperatures. For carbon, calculated and measured values are close to one another for FETA1 and FETA3 alloys, and the main mismatches exist for FETA2, with an inversion of order between 1000 and 1200°C.

##### 4.3. Computed mass fractions of carbides

Figure 6 shows the positions of the three alloys in isothermal sections of the Fe-30wt.%Cr-xC-yTa phase diagram at T=1200°C, 1100°C and 1000°C while Table 3 displays the calculated mass fractions of the existing carbides computed by Thermo-Calc and their corresponding volume fractions. There are two types of experimental values of the carbides volume fractions: the first one is the volume fraction of TaC deduced from the tantalum content of the matrix according to equations (1) and (2), while the second one (**in bold characters**) is the surface fraction measured by image analysis on the samples after exposure to the considered temperature.

It appears that some disagreement exists about the existence of the chromium carbides in FETA1. Indeed, calculations show that no chromium carbides do not exist at 1200°C or 1100°C while Cr<sub>23</sub>C<sub>6</sub> carbides appear at 1000°C, with a low fraction. The experiments show chromium carbides at 1200°C. At this temperature Cr<sub>23</sub>C<sub>6</sub> carbides become clearly visible. The mismatch is more serious for the TaC carbides: they always exist according both to calculations and to observations, but the surface fractions measured on samples by image analysis is largely greater than what is calculated by Thermo-Calc. The difference between the two decreases when exposure temperature increases from 1000°C (ratio of 10) to 1200°C (ratio of 3).

According to calculations performed for FETA2 alloy, chromium carbides would exist for the three temperatures and they are all of the Cr<sub>23</sub>C<sub>6</sub> type. An excellent agreement exists for 1200°C between calculation and image analysis for this alloy, while the calculated volume fractions are significantly greater than the measured surface fractions (ratio of about 3) for 1100 and 1000°C. This order is inversed for TaC carbides which are present in samples with a greater surface fraction than the calculated volume fractions, with a ratio of 2 at 1200°C up to a ratio of more than 3 for 1000°C.

Calculations show that no chromium carbides would appear in the FETA3 alloy whatever the exposure temperature, while TaC surface fractions in real samples are significantly greater again than predicted by Thermo-Calc (ratio of 2 or 3) at all temperatures.

Thus, image analysis led to carbide volume fractions (supposed equal to surface fractions) that have often great mismatches with calculations. TaC volume fractions obtained by image analysis are systematically higher than what comes from calculations, but the calculations/experiments correspondence is obviously better when the volume fractions deduced from the tantalum contents of both alloy and its matrix are considered: for all alloys and all temperatures they are very close to one another. About the chromium carbides, the same stoichiometry is obtained from calculations and from microanalysis but they are also mismatches between the calculated volume fractions and the experimental ones. Similarly as with TaC carbides, the correspondence is also improved when it is the chromium carbides volume fractions deduced from the matrix composition are considered. The agreement is not so good as for TaC carbides, what is probably due to a too light decreasing of the matrix Cr content compared to the Cr content in the whole alloy when chromium carbides are present.

## 5. Discussion

Tantalum, that is present in the studied alloys with about the same atomic content as carbon (FETA1 and FETA3) and half this content (FETA2), leads to a high density of tantalum carbides, than in Co-base alloys [13] or Ni-base alloys [14], what is clearly observed when the microstructures are examined using SEM in BSE mode. However image analysis performed on BSE pictures sometimes gives values of the TaC surface fractions that are obviously overestimated. A good example is the case of the FETA1 alloy which, according to surface fractions measurements, seems containing more TaC carbides after exposure at 1000°C than the FETA2 alloy, while the comparison between the two sets of pictures rather shows that the density of the TaC phase is similar in the two alloys. This can be explained by the high average atomic

number of these TaC carbides that induces a white colour that comes from the part of the TaC carbides that is just under the observed surface, as well as from the TaC part that really emerges on surface. Then image analysis, for which it is difficult to separate the two parts of the TaC carbides, leads to higher results than really observed. Another explanation for these differences is that it cannot be always assumed that surface fractions and volume fractions are almost equal: this can depend on the shape and the repartition of the considered particles. The assessment of carbides mass fractions and volume fractions can be made with a higher accuracy by determination from the chemical composition of the matrix that can be measured with a high precision using a WDS microprobe. It is the reason why only the results obtained for the TaC carbides by this second method are thereafter considered and compared to Thermo-Calc calculations.

During an exposure to 1000°C for 50 hours, no real microstructural changes occur in the alloys compared to the initial microstructures. It is not the case for 1100 and 1200°C for what TaC tends to partially disappear while new acicular (and more or less coarse) chromium carbides develop through the microstructure. These microstructural evolutions with temperature were not predicted by thermodynamic calculations for which no chromium carbides will appear in FETA1 and FETA3. For FETA2 calculations logically showed that such chromium carbides must exist, that is a logical consequence of an increased carbon content for a fixed tantalum content compared to FETA1. But the correspondence is never good for this FETA2 alloy since calculated values are significantly higher than the measured ones.

The volume fractions of TaC deduced from the tantalum contents of matrix and of the whole alloy stay almost constant when temperature varies between 1000 and 1200°C. There is a good correspondence between values deduced from alloy and matrix Ta content differences, and calculations. Thus, the best way to quantitatively get real TaC volume fractions on samples is really to calculate them from the Ta content differences between matrix and the whole alloy.

The solidus temperature of these Fe-base alloys are particularly high, compared to the corresponding Co-base and Ni-base alloys. Indeed, the FETA1 and FETA3 alloys show solidus temperatures that are about one hundred degrees over the corresponding Co-base and Ni-base alloys ones (for which the solidus temperatures are about 1300°C). Indeed, fusion of the FETA2 alloy, which begins by the fusion of the Cr<sub>23</sub>C<sub>6</sub>-matrix eutectic, leads to a lower solidus temperature. There is a small mismatch between experiments and calculations for the FETA1 and FETA2 alloys (about 20°C if the beginning of fusion is considered). Moreover the computed solidus temperature of the FETA3 alloy is sensibly higher than the one determined by thermal analysis.

Thus, comparisons between experiment and calculations also led to mismatches concerning the chromium carbides volume fractions, and for the solidus temperature for a high Ta content. The database must obviously be improved by the descriptions of new systems involving the TaC phase, i.e. be enriched with the lacking binary and ternary systems (Fe-Ta, Fe-Cr-Ta, Fe-C-Ta, ...).

## 6. Conclusions

These tantalum chromia-forming iron base alloys contain a significant amount of TaC carbides which can be very useful for mechanical strength at high temperature.

Moreover two of them appear as being particularly refractory with their very high solidus temperatures. Unfortunately they are obviously affected by some microstructural evolutions when exposed to high temperatures, that lead to a great reduction of the TaC volume fraction as well as the appearance of very coarse and acicular chromium carbides which may deteriorate mechanical properties. Thus, despite of several advantages for high temperature applications, it seems that such alloys cannot be always well adapted to be used as high temperature materials as conventionally cast superalloys.

Some thermal analysis and microstructural results correspond well to calculation results but they are also some disagreements between experimental results and computed predictions. The results obtained on these three real alloys can be of help to improve the databases concerning this quaternary Fe-Cr-C-Ta system. Indeed, the DTA results, the WDS compositions of the matrix and both nature and measured fractions of carbides (deduced from the Ta content of the matrix in the case of the TaC carbides) can be considered as targets to reach by calculations, for example for the assessment of the efficiency of modified databases. In a second article [15] the case of Fe-Ni-Cr-C-Ta alloys will be studied following the same method.

## Acknowledgements

The authors thank the Microanalysis Common Service of the Faculty of Sciences and Techniques of Nancy, especially Johann Ravaux and Alain Kohler.

## References

- [1] E. F. Bradley, *Superalloys: A Technical Guide*, ASM International, 1988.
- [2] C. T. Sims, W. C. Hagel, *The Superalloys*, John Wiley & Sons, 1972.
- [3] J.P. Mercier, G. Zambelli, W. Kurz, *Introduction à la science des matériaux*, Presses Polytechniques et Universitaires Romandes, 2002.
- [4] *Handbook of Chemistry and Physics*, 57<sup>th</sup> edition (1976-1977).
- [5] Thermo-Calc version N: "Foundation for Computational Thermodynamics" Stockholm, Sweden, Copyright (1993, 2000). [www.thermocalc.com](http://www.thermocalc.com)
- [6] SGTE: "Scientific Group Thermodata Europe" database, update 1992. [www.SGTE.org](http://www.SGTE.org)
- [7] P. Gustafson, *Scan. J. Metall.* 14 (1985) 259-264.
- [8] J.O. Anderson, B. Sundman, *CALPHAD* 11 (1987) 83-92.
- [9] J.O. Anderson, *CALPHAD* 11 (1987) 271-276.
- [10] J.O. Anderson, *Met. Trans. A* 19A (1988) 627-636.
- [11] K. Frisk and A. Fernandez Guillermet, *J. Alloys and Compounds* 238 (1996) 167-179.
- [12] N. Dupin and I. Ansara, *J. Phase Equilibria* 14 (1993) 451-456.
- [13] P. Berthod, S. Michon, L. Aranda, S. Mathieu and J.C. Gachon, *CALPHAD* 27 (2003) 353-359.
- [14] P. Berthod, L. Aranda, C. Vébert, S. Michon *CALPHAD*, 28 (2004) 159-166.
- [15] P. Berthod, Y. Hamini, L. Hélicher, L. Aranda, submitted to *CALPHAD*.

## TABLES

Table 1  
Chemical compositions of the studied alloys, targeted and obtained (**in bold characters**)  
(average values of EDS measurements performed on three x250 areas)

Alloy	Chemical Composition	Fe	Cr	Ta	C
<b>FETA1</b>	targeted	bal.	30	3	0.2
	<b>obtained</b>	<b>bal.</b>	<b>29.8</b> +/- 0.7	<b>2.1</b> +/- 0.5	Supposed to be <b>0.2</b>
<b>FETA2</b>	targeted	bal.	30	3	0.4
	<b>obtained</b>	<b>bal.</b>	<b>29.5</b> +/- 2.7	<b>2.4</b> +/- 0.4	Supposed to be <b>0.4</b>
<b>FETA3</b>	targeted	bal.	30	6	0.4
	<b>obtained</b>	<b>bal.</b>	<b>29.2</b> +/- 1.6	<b>6.2</b> +/- 1.1	Supposed to be <b>0.4</b>

Table 2  
Solidus and liquidus temperatures of the three alloys  
measured by Differential Thermal Analysis (**in bold characters**) and computed by  
ThermoCalc

Alloy	Solidus Temp. (°C)	Liquidus Temp. (°C)
	<b>DTA: heating only (average heating/cooling)</b> Thermo-Calc	
FETA1	<b>1419 (1408)</b>	<b>&gt;1500°C (&gt;1500°C)</b>
	1436	1525
FETA2	<b>1320 (1302)</b>	<b>&gt;1500°C (&gt;1500°C)</b>
	1298	1563
FETA3	<b>1405 (1390)</b>	<b>&gt;1500°C (&gt;1500°C)</b>
	1471	1713

Table 3

Surface fractions of carbides measured using image analysis performed on SEM-BSE pictures for each alloy and each temperature (**in bold characters**); comparison with volume fractions deduced from the Cr and Ta contents of the matrix (normal characters) and with volume fractions calculated using Thermo-Calc (*italic characters*)

Alloy	<i>calculated volume fractions (%)</i> , vol. fract. from %Cr and %Ta in matrix (%) <b>and surface fractions (%)</b>	M <sub>23</sub> C <sub>6</sub>	TaC
<b>FETA1</b>  <b>1200°C</b>	(calculated mass fractions) <i>calculated volume fractions</i>	0 <i>0</i>	2.17 <i>1.15</i>
	vol. frac. deduced from matrix %Cr and %Ta	0	1.12
	<b>measured by image analysis</b>	<b>1.98</b> +/-0.36	<b>3.41</b> +/-0.24
<b>FETA1</b>  <b>1100°C</b>	(calculated mass fractions) <i>calculated volume fractions</i>	0 <i>0</i>	2.24 <i>1.19</i>
	deduced from matrix %Cr and %Ta	0	1.16
	<b>measured by image analysis</b>	<b>0.13</b> +/-0.02	<b>4.11</b> +/-0.29
<b>FETA1</b>  <b>1000°C</b>	(calculated mass fractions) <i>calculated volume fractions</i>	0.44 <i>0.48</i>	2.26 <i>1.20</i>
	deduced from matrix %Cr and %Ta	0.30	1.17
	<b>measured by image analysis</b>	<b>0.06</b> +/-0.04	<b>10.71</b> +/-0.59
<b>FETA2</b>  <b>1200°C</b>	(calculated mass fractions) <i>calculated volume fractions</i>	2.23 <i>2.47</i>	2.54 <i>1.35</i>
	deduced from matrix %Cr and %Ta	1.26	1.32
	<b>measured by image analysis</b>	<b>2.46</b> +/-0.54	<b>2.70</b> +/-0.61
<b>FETA2</b>  <b>1100°C</b>	(calculated mass fractions) <i>calculated volume fractions</i>	3.11 <i>3.44</i>	2.57 <i>1.36</i>
	deduced from matrix %Cr and %Ta	2.08	1.33
	<b>measured by image analysis</b>	<b>1.19</b> +/-0.51	<b>5.17</b> +/-0.91
<b>FETA2</b>  <b>1000°C</b>	(calculated mass fractions) <i>calculated volume fractions</i>	3.68 <i>4.06</i>	2.58 <i>1.36</i>
	deduced from matrix %Cr and %Ta	2.57	1.34
	<b>measured by image analysis</b>	<b>1.44</b> +/-0.71	<b>4.57</b> +/-1.32
<b>FETA3</b>  <b>1200°C</b>	(calculated mass fractions) <i>calculated volume fractions</i>	0 <i>0</i>	6.29 <i>3.40</i>
	deduced from matrix %Cr and %Ta	0	3.32
	<b>measured by image analysis</b>	<b>3.45</b> +/-0.71	<b>6.36</b> +/-1.35
<b>FETA3</b>  <b>1100°C</b>	(calculated mass fractions) <i>calculated volume fractions</i>	0 <i>0</i>	6.42 <i>3.47</i>
	deduced from matrix %Cr and %Ta	0	3.39
	<b>measured by image analysis</b>	<b>3.86</b> +/-2.51	<b>6.93</b> +/-0.31
<b>FETA3</b>  <b>1000°C</b>	(calculated mass fractions) <i>calculated volume fractions</i>	0 <i>0</i>	6.50 <i>3.52</i>
	deduced from matrix %Cr and %Ta	0.04	3.44
	<b>measured by image analysis</b>	<b>0.07</b> +/-0.15	<b>9.50</b> +/-0.96

Table 4  
 Matrix chemical compositions at 1000°C, 1100°C and 1200°C,  
 analysed with WDS microprobe (**in bold characters**) and computed with Thermo-Calc

Alloy	Fe	Cr	Ta	C
		<b>Weight contents analysed by microprobe (%)</b> Calculated weight contents (%)		
<b>FETA1</b>				
<b>1200°C</b>	<b>bal.</b>	<b>29.9 +/- 0.2</b> 30.5	<b>0.05 +/- 0.04</b> 0.11	<b>0</b> 0.07
<b>1100°C</b>	<b>bal.</b>	<b>30.7 +/- 0.1</b> 30.5	<b>0.06 +/- 0.05</b> 0.04	<b>0.08 +/- 0.08</b> 0.06
<b>1000°C</b>	<b>bal.</b>	<b>29.9 +/- 1.6</b> 30.3	<b>0.04 +/- 0.05</b> 0.02	<b>0.11 +/- 0.10</b> 0.04
<b>FETA2</b>				
<b>1200°C</b>	<b>bal.</b>	<b>30.6 +/- 0.2</b> 29.5	<b>0.02 +/- 0.03</b> 0.06	<b>0.02 +/- 0.02</b> 0.12
<b>1100°C</b>	<b>bal.</b>	<b>29.7 +/- 0.2</b> 29.0	<b>0.05 +/- 0.04</b> 0.04	<b>0.01 +/- 0.02</b> 0.07
<b>1000°C</b>	<b>bal.</b>	<b>30.7 +/- 0.1</b> 28.7	<b>0.05 +/- 0.05</b> 0.02	<b>0.17 +/- 0.03</b> 0.04
<b>FETA3</b>				
<b>1200°C</b>	<b>bal.</b>	<b>30.9 +/- 0.6</b> 31.2	<b>0.07 +/- 0.03</b> 0.34	<b>0</b> 0.02
<b>1100°C</b>	<b>bal.</b>	<b>31.9 +/- 0.15</b> 31.2	<b>0.07 +/- 0.02</b> 0.21	<b>0.01 +/- 0.01</b> 0.01
<b>1000°C</b>	<b>bal.</b>	<b>33.1 +/- 0.2</b> 31.2	<b>0.06 +/- 0.04</b> 0.12	<b>0</b> 0.01

## FIGURES

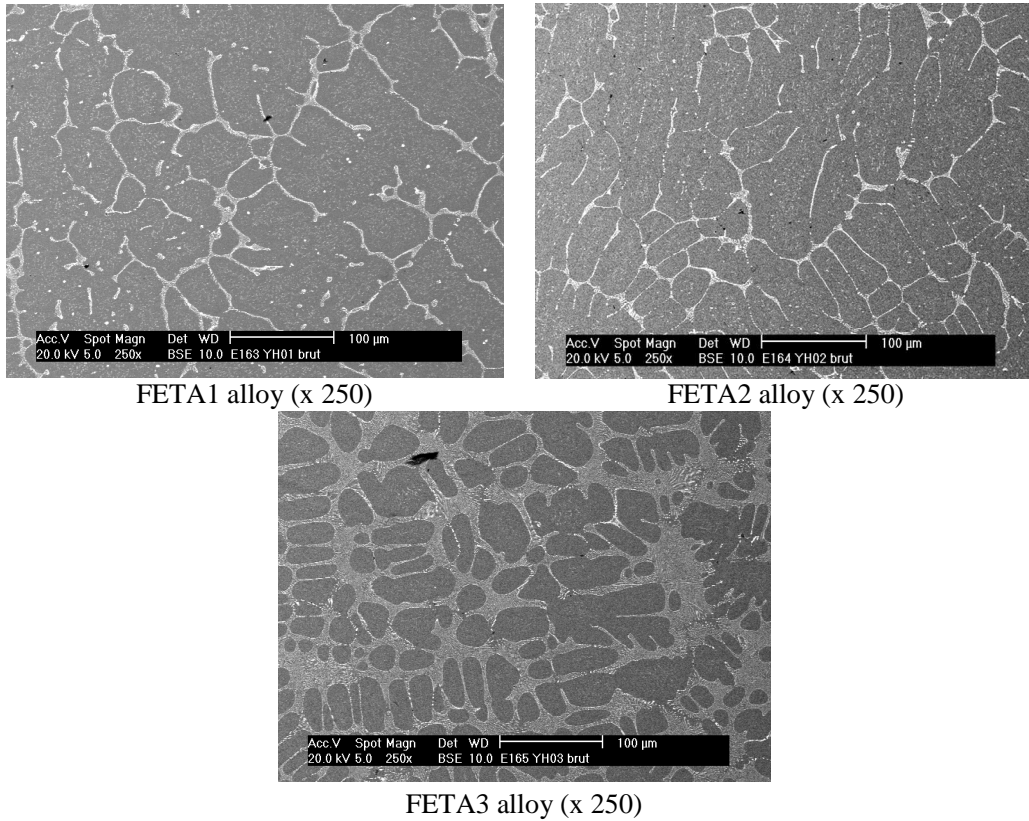


Fig. 1. Initial microstructures of the three alloys (after solidification and stress-releasing heat treatment) (all pictures taken with MEB in BSE mode)

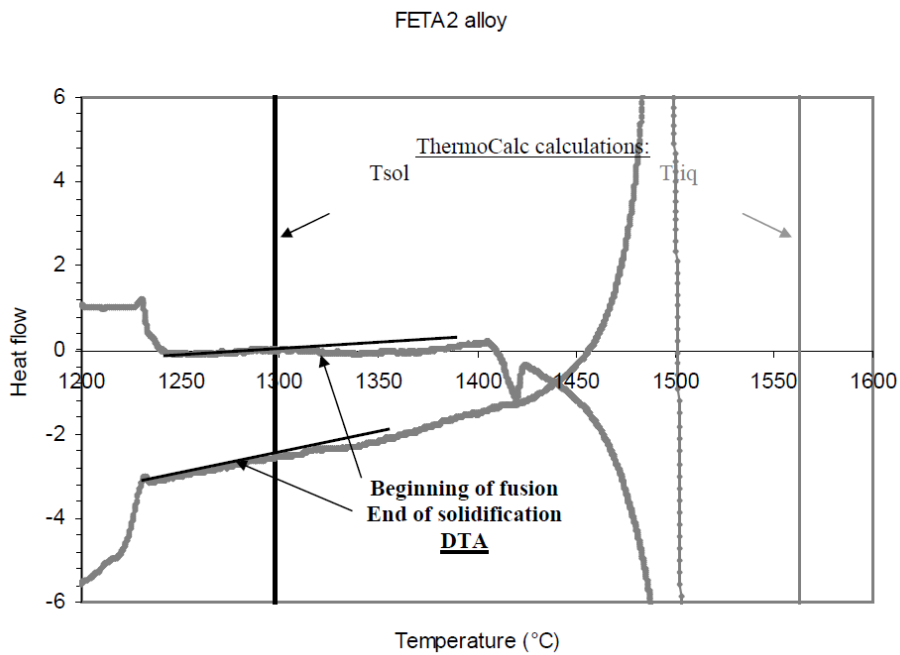
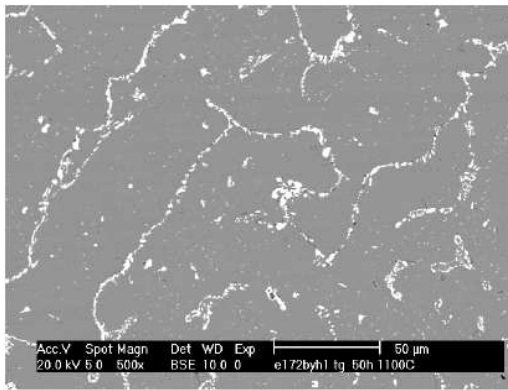
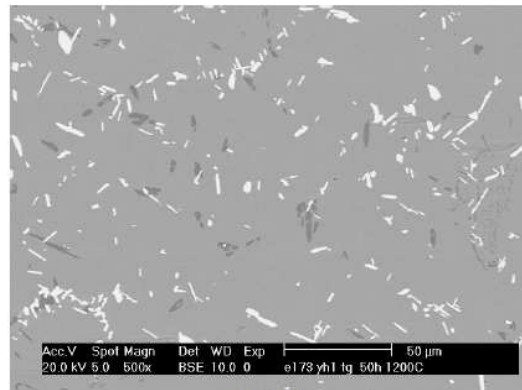


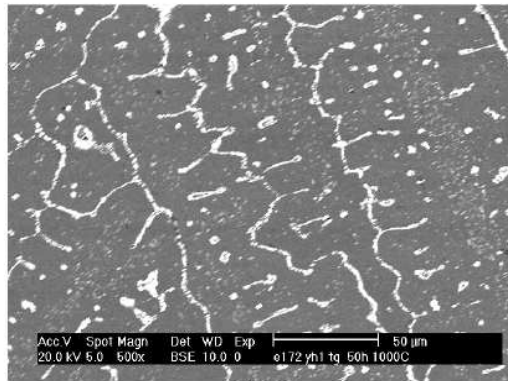
Fig. 2. An example of a DTA curve with determination of the temperatures of the beginnings and ends of fusion and solidification respectively (here FETA2 alloy)



1100°C

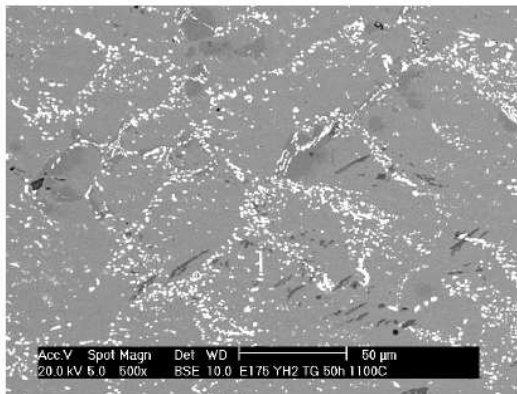


1200°C

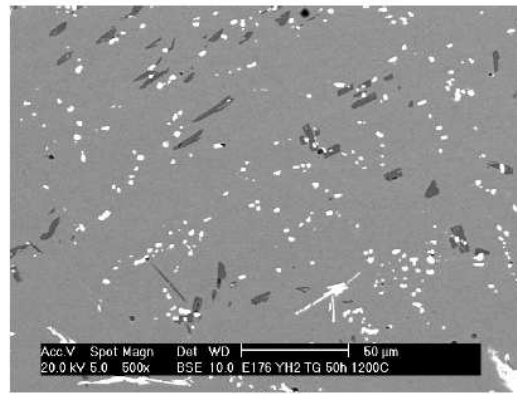


1000°C

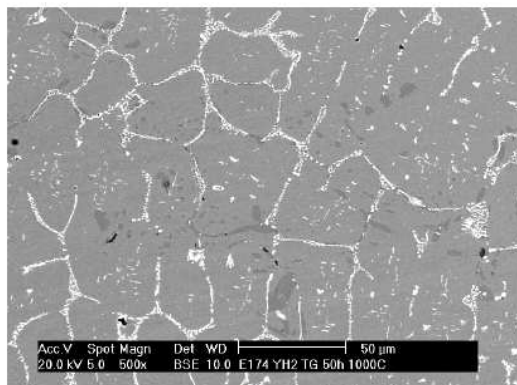
Fig. 3. Stable microstructures of FETA1 alloy after 50 hours-exposure at 1000°C, 1100°C and 1200°C (all pictures taken with MEB in BSE mode at x500)



1100°C

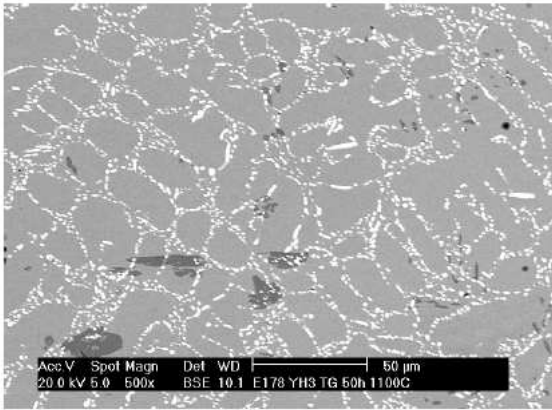


1200°C

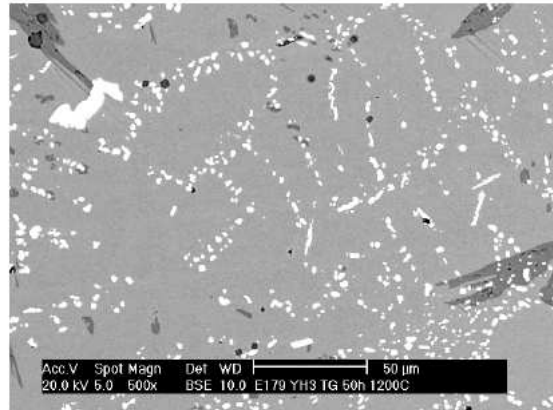


1000°C

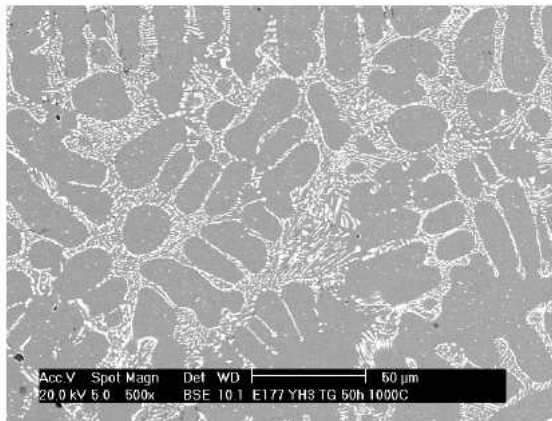
Fig. 4. Stable microstructures of FETA2 alloy after 50 hours-exposure at 1000°C, 1100°C and 1200°C (all pictures taken with MEB in BSE mode at x500)



1100°C



1200°C



1000°C

Fig. 5. Stable microstructures of FETA3 alloy after 50 hours-exposure at 1000°C, 1100°C and 1200°C (all pictures taken with MEB in BSE mode at x500)

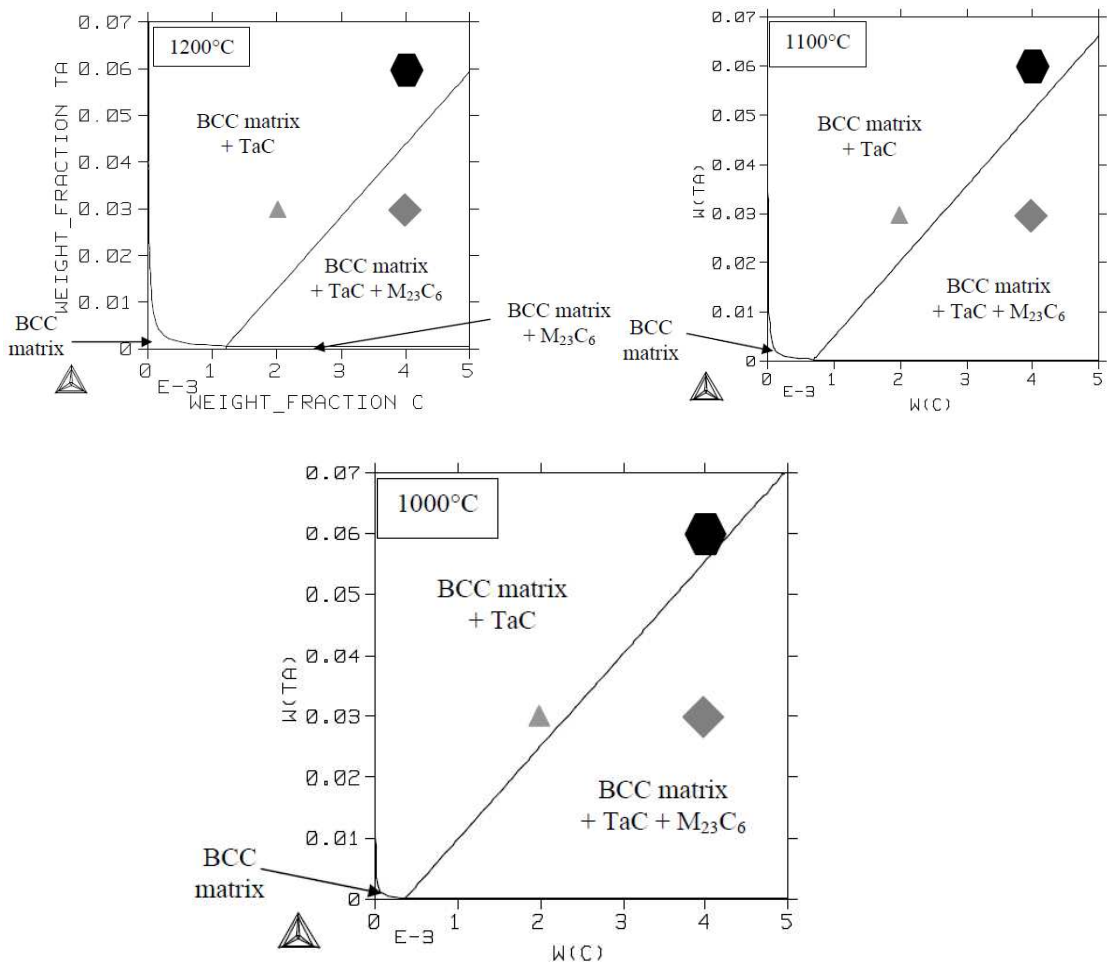


Fig. 6. Isothermal sections of the Fe-30wt.%Cr-xC-yTa phase diagram with positions of the three alloys: FETA1 ( $\blacktriangle$ ), FETA2 ( $\blacklozenge$ ) and FETA3 ( $\blackhexagon$ )